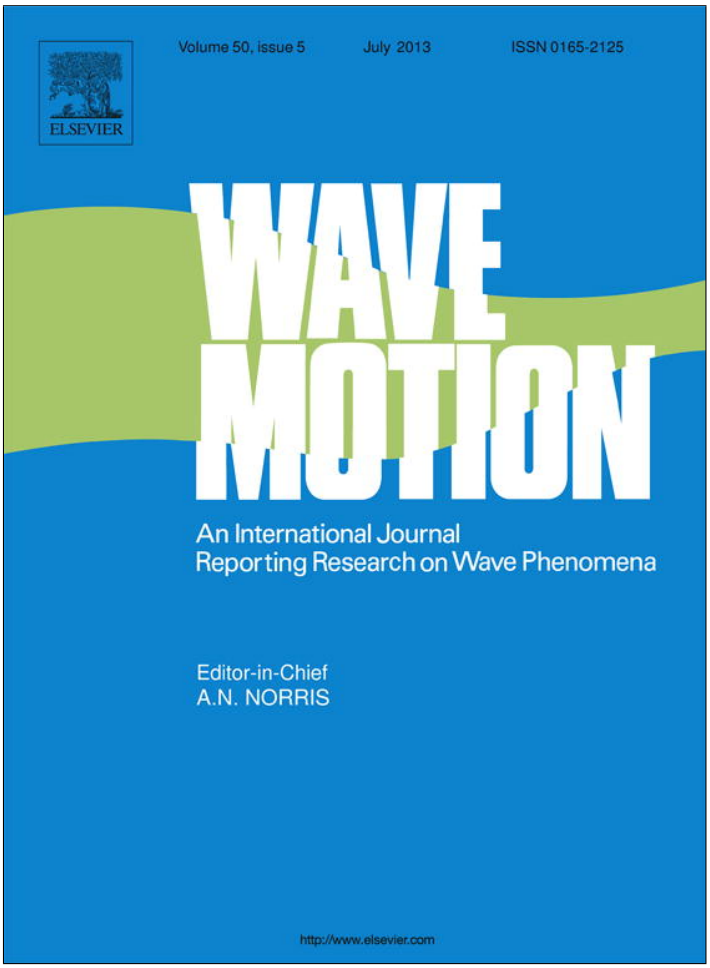

Wave Motion 50 (2013) 929–939

Contents lists available at SciVerse ScienceDirect

Wave Motion

journal homepage: www.elsevier.com/locate/wavemoti

Progressive waves in a compressible-ocean with an elastic bottom

Erez Eyov, Assaf Klar, Usama Kadri *, Michael Stiassnie

Faculty of Civil and Environmental Engineering, Technion - Israel Institute of Technology, Haifa 32000, Israel

HIGHLIGHTS

- The leading acoustic-gravity mode dominates the solution.
- At large enough depths, the solution for the leading mode is only slightly affected by the elasticity of the ground.
- At relatively small water depths only the Scholte wave outlasts.
- Light is shed on mechanisms involved in transforming energy from the ocean to the crust as part of the microseisms phenomenon.
- The depth at which an acoustic-gravity wave attains its maximum intensity can be estimated.
- Knowledge of the behavior of acoustic-gravity waves with depth can be applied for the early detection of tsunami.

ARTICLE INFO

Article history:
Received 24 December 2012
Accepted 9 March 2013
Available online 28 March 2013

Keywords:
Acoustic gravity wave
Elastic seabed
Microseisms
Tsunami

ABSTRACT

The mathematical solution for the two-dimensional linear problem of acoustic-gravity waves in a compressible ocean with an elastic bottom is presented. The physical properties of these waves are studied, and compared with those for waves over rigid ground. The solutions for constant water depth, together with the assumption of constant energy flux, are used to study the shoaling of acoustic-gravity waves over a slowly-varying bathymetry. The present work enriches our knowledge about acoustic-gravity waves in a way that could assist, among others, in the early detection of tsunami.

1. Introduction

Most studies of ocean surface-waves neglect the small compressibility of the water. This approach is justified for many physical applications, but not necessarily for all. In an incompressible ocean, with constant depth, h, and rigid-bottom, any given frequency ω corresponds to one progressive *gravity* wave with wavenumber k. If the small compressibility of the water is taken into account, any given frequency ω corresponds to several progressive waves, with wavenumbers $k_n, n = 0, 1, \ldots, N$. The wavenumber k_0 is almost identical to k, whereas $k_N < k_{N-1} < \cdots < k_2 < k_1 \ll k_0$. The additional waves $(k_1, \ldots, k_N)$ are called *acoustic-gravity* waves, and N is the nearest integer smaller than $(\omega h/\pi C_l + 1/2)$, where C_l is the speed of sound in water.

Acoustic-gravity waves are generated spontaneously in the ocean, as a result of nonlinear interactions of pairs of nearly opposing gravity-waves having equal or nearly equal frequencies, see [1–3], and references therein. Particularly energetic acoustic-gravity waves appear as a result of submarine earthquake, see [4, Chapter 3].

In contrast to the gravity wave, which decays exponentially with depth, the acoustic-gravity waves have an oscillatory vertical profile down to the ocean bottom, which stresses the ground and generates the earth's microseism [5]. In this note

* Corresponding author. Tel.: +972 48292580.
E-mail address: usama.kadri@gmail.com (U. Kadri).

0165-2125/$ – see front matter © 2013 Elsevier B.V. All rights reserved.
http://dx.doi.org/10.1016/j.wavemoti.2013.03.003

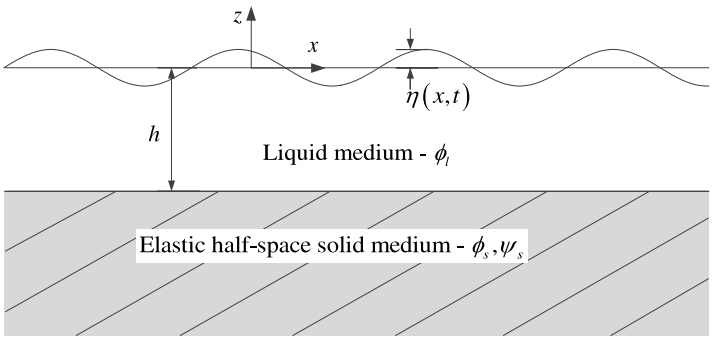

Fig. 1. Schematic representation of the flow domain; h is the water depth; $\eta(x, t)$ is the surface elevation; ϕ_l is the velocity potential of the liquid medium; ϕ_s and ψ_s are the dilatation and rotation potentials of the half-space solid medium, respectively.

we study the effects of replacing the rigid-bottom assumption, by an elastic half-space solid medium, on the properties of the acoustic-gravity waves.

This paper is composed of five main sections. The physical problem is formulated in Section 2 and its mathematical solution is given in Section 3. The results for water of constant depth, and for waves shoaling over a slowly varying bathymetry are discussed in Sections 4 and 5, respectively. Finally, conclusions are drawn in Section 6.

2. Formulation

Let us consider an ocean of a constant depth-h, in the field of gravity-g, assume that it is unbounded in the horizontal x-direction and supported below by an infinite deep elastic solid. The origin of the Cartesian coordinate system is at the unperturbed free-surface and the z-axis is oriented upwards, see Fig. 1.

The study of two-dimensional progressive waves is formulated herein by

(i) The linearized theory of irrotational flow for the liquid.
(ii) Linear elasticity theory for the solid.

The velocity components of the liquid in the-(x, z) directions are denoted by $(\dot{u}_l, \dot{w}_l)$, whereas the corresponding displacements in the solid are (u_s, w_s). These kinematic quantities can be expressed through: (i) a velocity potential ϕ_l, for the liquid; and (ii) a dilatation potential ϕ_s and a rotation potential ψ_s, for the solid. The kinematic quantities are related to the potentials by

$$\dot{u}_l = -\frac{\partial \phi_l}{\partial x}, \tag{1a}$$

$$\dot{w}_l = -\frac{\partial \phi_l}{\partial z}, \tag{1b}$$

$$u_s = \frac{\partial \phi_s}{\partial x} + \frac{\partial \psi_s}{\partial z}, \tag{2a}$$

$$w_s = \frac{\partial \phi_s}{\partial z} - \frac{\partial \psi_s}{\partial x}. \tag{2b}$$

The potentials themselves are governed by three wave-equations,

$$\frac{\partial^2 \phi_l}{\partial t^2} = C_l^2 \left(\frac{\partial^2 \phi_l}{\partial x^2} + \frac{\partial^2 \phi_l}{\partial z^2} \right), \quad -h \le z \le 0, \tag{3}$$

$$\frac{\partial^2 \phi_s}{\partial t^2} = C_p^2 \left(\frac{\partial^2 \phi_s}{\partial x^2} + \frac{\partial^2 \phi_s}{\partial z^2} \right), \quad z \le -h, \tag{4}$$

and

$$\frac{\partial^2 \psi_s}{\partial t^2} = C_s^2 \left(\frac{\partial^2 \psi_s}{\partial x^2} + \frac{\partial^2 \psi_s}{\partial z^2} \right), \quad z \le -h, \tag{5}$$

where C_l is the speed of sound in the water; and C_p, C_s are the pressure-wave and shear-wave velocities in the ground, respectively. Note that, the later two maybe related to the Lame's elasticity constants (λ, μ) and the density of the solid (ρ_s) by:

$$C_p = \sqrt{(\lambda + 2\mu)/\rho_s}, \tag{6a}$$

$$C_s = \sqrt{\mu/\rho_s}. \tag{6b}$$

To complete the mathematical formulation one has to specify the boundary conditions at the free surface, at the bottom and at $z \to -\infty$. The linearized free-surface boundary condition is

$$\frac{\partial^2 \phi_l}{\partial t^2} + g\frac{\partial \phi_l}{\partial z} = 0, \quad z = 0. \tag{7}$$

At the bottom one has three conditions,

$$\frac{\partial w_s}{\partial t} = \dot{w}_l, \quad z = -h, \tag{8a}$$

$$\sigma_{zz} = -P_l, \quad z = -h, \tag{8b}$$

and

$$\sigma_{xz} = 0, \quad z = -h, \tag{8c}$$

where the axial-stress σ_{zz} and shear-stress σ_{xz} are given by

$$\sigma_{zz} = \lambda\left(\frac{\partial u_s}{\partial x} + \frac{\partial w_s}{\partial z}\right) + 2\mu\frac{\partial w_s}{\partial z}, \tag{9a}$$

$$\sigma_{xz} = \mu\left(\frac{\partial w_s}{\partial x} + \frac{\partial u_s}{\partial z}\right), \tag{9b}$$

and the dynamic pressure in the water is

$$P_l = \rho_l\frac{\partial \phi_l}{\partial t}, \tag{10}$$

where ρ_l is the density of the water.

For $z \to -\infty$ we require that ϕ_s and ψ_s decay. Note that the free-surface elevation is given by

$$\eta = \frac{1}{g}\frac{\partial \phi_l}{\partial t}, \quad z = 0. \tag{11}$$

3. Solution

Seeking progressive wave solutions, using the method of separation of variables and the condition at $z \to -\infty$, one gets

$$\phi_s = D_1 \exp\left(qz + i(kx - \omega t)\right), \tag{12a}$$

$$\psi_s = D_2 \exp\left(sz + i(kx - \omega t)\right), \tag{12b}$$

and

$$\phi_l = \left[E_1 \cos(irz) + E_2 \sin(irz)\right] \exp\left(i(kx - \omega t)\right), \tag{12c}$$

where ω is a prescribed frequency, and

$$q = \sqrt{k^2 - \omega^2/C_p^2}, \tag{13a}$$

$$s = \sqrt{k^2 - \omega^2/C_s^2}, \tag{13b}$$

$$r = \sqrt{k^2 - \omega^2/C_l^2}, \tag{13c}$$

and k is the wavenumber, which needs to be solved.

The constants D_1, D_2 and E_1, E_2 are obtained as follows. Using the boundary conditions prescribed by Eqs. (7) and (8c), gives respectively

$$E_2 = -i\omega^2 E_1/(gr), \tag{14a}$$

$$D_2 = -2ikq \exp\left(h(s - q)\right) D_1/(k^2 + s^2). \tag{14b}$$

Substituting Eq. (14b) into Eqs. (12b) and (14a) into Eq. (12c) and then Eqs. (12a)–(12c) into the remaining boundary conditions, Eqs. (8a) and (8b), gives a homogeneous system of two linear algebraic equations for two unknowns D_1, E_1

$$\begin{aligned} a_{11}D_1 + a_{12}E_1 &= 0, \\ a_{21}D_1 + a_{22}E_1 &= 0, \end{aligned} \tag{15}$$

where

$$a_{11} = i\omega q \exp(-qh)(k^2 - s^2)/(k^2 + s^2), \tag{16a}$$

$$a_{12} = ir \sin(irh) + \omega^2 \cos(irh)/g, \tag{16b}$$

$$a_{21} = \exp(-qh)\left(4\mu k^2 sq/(k^2 + s^2) - (\lambda + 2\mu)q^2 + \lambda k^2\right), \tag{16c}$$

$$a_{22} = \omega\rho_l\left(i\cos(irh) - \omega^2 \sin(irh)/(gr)\right). \tag{16d}$$

For a nontrivial solution, the determinant of Eq. (15) must vanish, which yields the following dispersion relation,

$$\tanh(hr) = \frac{\frac{\omega^2}{r}\left(q\rho_l\left(\frac{k^2-s^2}{k^2+s^2}\right) + \frac{1}{g}\left(\frac{4k^2qs\mu}{k^2+s^2} - \left((\lambda+2\mu)\,q^2 - \lambda k^2\right)\right)\right)}{\frac{\omega^4 q\rho_l}{gr^2}\left(\frac{k^2-s^2}{k^2+s^2}\right) + \left(\frac{4k^2qs\mu}{k^2+s^2} - \left((\lambda+2\mu)\,q^2 - \lambda k^2\right)\right)}. \tag{17}$$

Note that substitution of Eqs. (13a)–(13c) into Eq. (17) enables to view the latter either in the form of $k = k(\omega, g, \rho_l, \rho_s, \lambda, \mu)$ or alternatively as, $r = r(\omega, g, \rho_l, \rho_s, \lambda, \mu)$. In addition Eq. (15), gives

$$D_1 = -a_{12}E_1/a_{11}, \tag{18}$$

and Eq. (11) yields

$$\eta = -i\omega/gE_1 \exp\left(i(kx - \omega t)\right) \equiv A \exp\left(i(kx - \omega t)\right), \tag{19}$$

where

$$A = -i\omega E_1/g, \tag{20a}$$

or

$$E_1 = -igA/\omega. \tag{20b}$$

Eqs. (20b), (18), (14a) and (14b), enable us to express all four unknowns E_1, E_2, D_1 and D_2 in terms of a freely chosen free-surface amplitude A. Writing the unknowns in terms of the free-surface amplitude A, gives

$$E_1 = igA/\omega, \tag{21a}$$

$$D_1 = -\frac{\exp(qh)\left(k^2 + s^2\right)\left(igr\sin(ihr) + \omega^2\cos(ihr)\right)}{q\omega^2\left(k^2 - s^2\right)}A, \tag{21b}$$

$$E_2 = \omega A/r, \tag{21c}$$

$$D_2 = \frac{2ik\exp(sh)\left(igr\sin(ihr) + \omega^2\cos(ihr)\right)}{\omega^2\left(k^2 - s^2\right)}A. \tag{21d}$$

By substituting Eqs. (21b) and (21d) into Eqs. (12a) and (12b), and Eqs. (21a) and (21c) into Eq. (12c), we can express the potential functions in terms of A,

$$\phi_s = -\frac{\exp\left(q(h+z)\right)\left(k^2 + s^2\right)\left(igr\sin(ihr) + \omega^2\cos(ihr)\right)}{q\omega^2\left(k^2 - s^2\right)}A\exp\left(i(kx - \omega t)\right), \tag{22a}$$

$$\psi_s = \frac{2ik\exp\left(s(h+z)\right)\left(igr\sin(ihr) + \omega^2\cos(ihr)\right)}{\omega^2\left(k^2 - s^2\right)}A\exp\left(i(kx - \omega t)\right), \tag{22b}$$

$$\phi_l = \left(ig/\omega\cos(irz) + \omega/r\sin(irz)\right)A\exp\left(i(kx - \omega t)\right). \tag{22c}$$

Substituting Eqs. (22a) and (22b) into Eq. (2a,b) and taking the real part, gives us the solid's horizontal and vertical displacement functions in terms of A as follows (note that for acoustic-gravity waves, r is always imaginary):

$$u_s = Ak\left(\frac{k^2 + s^2}{q}\exp\left(q(z+h)\right) - 2s\exp\left(s(z+h)\right)\right)\cdot\frac{igr\sin(ihr) + \omega^2\cos(ihr)}{\omega^2\left(k^2 - s^2\right)}\sin(kx - \omega t), \tag{23a}$$

$$w_s = A\left(2k^2\exp\left(s(z+h)\right) - \left(k^2 + s^2\right)\exp\left(q(z+h)\right)\right)\cdot\frac{igr\sin(ihr) + \omega^2\cos(ihr)}{\omega^2\left(k^2 - s^2\right)}\cos(kx - \omega t). \tag{23b}$$

Similarly, substituting Eq. (22a) into Eqs. (1a,b) and taking only the real part yields the liquid's horizontal and vertical velocities in terms of A, as follows

$$\dot{u_l} = Ak\left(g\cos(irz)/\omega - i\omega\sin(irz)/r\right)\cos(kx - \omega t), \tag{24a}$$

$$\dot{w_l} = -A\left(irg\sin(irz)/\omega - \omega\cos(irz)\right)\sin(kx - \omega t). \tag{24b}$$

Substituting Eqs. (23a) and (23b) into Eqs. (9a) and (9b), and taking the real part as before, gives

$$\sigma_{zz} = A\left(4\mu s k^2 \exp\left(s(z+h)\right) + \left(k^2+s^2\right)\left(\lambda k^2/q - (\lambda+2\mu)q\right)\exp\left(q(z+h)\right)\right) \cdot \frac{igr\sin(ihr) + \omega^2\cos(ihr)}{\omega^2\left(k^2-s^2\right)}\cos(kx-\omega t), \tag{25a}$$

$$\sigma_{xz} = 4A\mu k\left(k^2+s^2\right)\left(\exp\left(q(z+h)\right) - \exp\left(s(z+h)\right)\right)\cdot\frac{igr\sin(ihr)+\omega^2\cos(ihr)}{\omega^2\left(k^2-s^2\right)}\sin(kx-\omega t). \tag{25b}$$

In order to express the pressure, P_l, in term of A, one should substitute Eq. (22c) into Eq. (10) and take only the real part, as follows

$$P_l = A\rho_l\left(g\cos(irz) - i\omega^2/r\sin(irz)\right)\cos(kx-\omega t). \tag{26}$$

In addition, substituting $z=-h$ into Eq. (23b) yields the seabed vertical displacement function

$$w_s(z=-h) = A\left(igr\sin(ihr)/\omega^2 + \cos(ihr)\right)\cos(kx-\omega t). \tag{27}$$

4. Results for constant depth

For a rigid bottom the dispersion relation (17) simplifies to

$$\tanh(hr) = \frac{\omega^2}{gr}. \tag{28}$$

It can be shown that Eq. (28) has only one real root, and an infinite number of pure imaginary roots. The real root corresponds to the well-known gravity wave, whereas the first few imaginary roots can produce progressive acoustic-gravity waves, as discussed in the introduction. The more complicated structure of the dispersion relation (17) does not support such a simple picture, since it has not only real and pure imaginary roots, but also complex ones.

For our numerical examples we rely on average parameter-values taken from the entries for the crust and ocean in Table 1 of PREM, [6], as given below:

Densities: $\rho_l = 1020\ \mathrm{kg/m^3}$, $\rho_s = 2750\ \mathrm{kg/m^3}$

Speeds: $C_l = 1450\ \mathrm{m/s}$, $C_s = 3550\ \mathrm{m/s}$, $C_p = 6300\ \mathrm{m/s}$.

For the above mentioned parameters our numerical investigation indicates that the number of progressive modes for the problem with an elastic bottom, (for a wide range of depths and frequencies), is nearly the same as that of the problem with a rigid bottom.

We have chosen to present our results for two frequencies $\omega_1 = 1\ \mathrm{Hz} = 2\pi\ \mathrm{rad/s}$ and $\omega_2 = 0.167\ \mathrm{Hz}$, both within the microseism frequency range, see Fig. 1 in [7]. For ω_1 we cover the depths range (0,4000 m), and follow the behavior of four acoustic-gravity modes; whereas for ω_2 we present results for (0,8000 m), and study the variation of the two possible acoustic-gravity modes.

Figs. 2(a) and 3(a) give the variation of the phase-velocities $c = \omega/k$ of all possible progressive modes for the frequencies 1 Hz and 0.167 Hz, respectively. The dashed curves give the results for a rigid bottom, whereas the solid lines for an elastic bottom.

All phase-speeds increase with decreasing depth. For a given mode, the curves for the rigid bottom and for the elastic bottom are almost identical in their deeper part, but diverge at smaller water depth. All progressive modes for a rigid bottom terminate at the depth of

$$h_{rn} \simeq (n-0.5)\pi\frac{C_l}{\omega}, \quad n=1,2,\ldots \tag{29}$$

where the phase-velocities tend to infinity (the wavenumbers k tend to zero). All progressive modes for an elastic bottom, except the first $n=1$, terminate at the depth of

$$h_{en} = (n-1.5)\pi\frac{C_l C_s}{\omega(C_s^2-C_l^2)^{1/2}}, \quad n=2,3,\ldots \tag{30}$$

where the parameters $s=0$ and $c=C_s$, see (13b). The first progressive mode for the elastic bottom is actually a Scholte wave, see [8], which turns into a Rayleigh wave at the shoreline. The physical meaning of h_{rn} and h_{en} is discussed later.

The ratio of the ground-amplitude to the free-surface amplitude $w_s(z=-h)/\eta$ is obtained from Eqs. (27) and (19), and plotted in Figs. 2(b) and 3(b). From these figures it is clear that the vertical motions of the ground and of the free surface are of comparable size over the whole ocean. The orders of magnitude of these motions are from 10^{-6} m for microseisms, to 10^{-2} m for severe earthquakes; see [5] for the first, and [9] for the second. For a gravity wave with frequency 0.167 Hz the

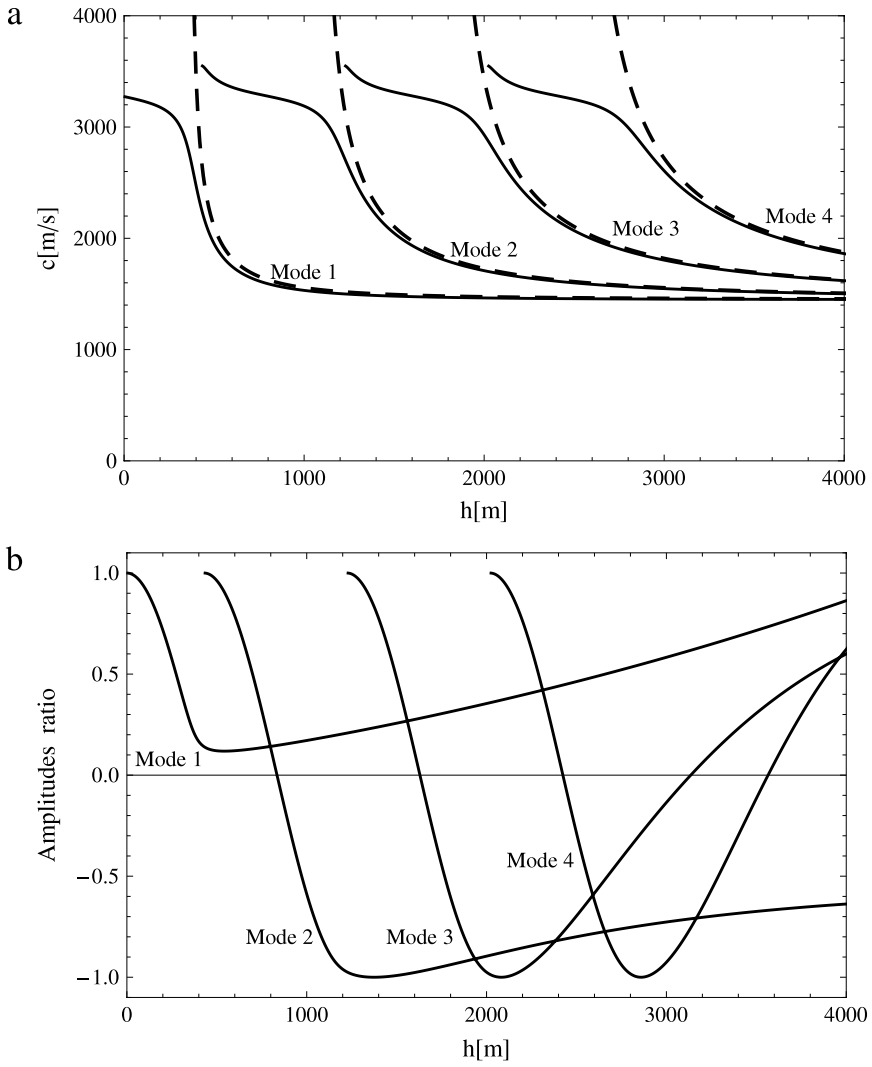

Fig. 2. Progressive acoustic-gravity modes with a frequency of 1 Hz. (a) variation of phase-velocity with depth. (b) variation of the ratio of the ground-amplitude to the free-surface-amplitude as a function of the water depth. Dashed curves: rigid bottom; solid curves: elastic bottom.

maximum ground-amplitude to free-surface amplitude ratio is reached at a depth of about 6 m and equals 2×10^{-6} which for a surface wave one meter high, gives a ground amplitude of 10^{-6} m, see Fig. 4.

5. Results for wave shoaling

The term *wave shoaling* refers to the two-dimensional problem (one horizontal dimension x) of waves propagating at normal incidence to straight parallel depth contours, usually in the shoreward direction. Assuming a slowly varying bathymetry, i.e. $(\mathrm{d}h/\mathrm{d}x)/(k_n h) \ll 1$; one can use a WKB approach, for which the constant depth solution is valid locally to obtain: (i) that $\omega = constant$, (thus k_n is given by the linear dispersion-relation); and (ii) that the energy-flux $F_n = constant$; see [10, Chapter 3].

The energy flux is the product of the energy density E_n and the group-velocity $c_{g,n}$ (to be distinguished from the phase velocity $c_n = \omega/k_n$).

For gravity waves, both $c_{g,0}$ and c_0 are real for any depth, and tend to zero as the depth h tends to zero. As a result, the wave-steepness tends to infinity and gravity waves break in coastal-waters (usually with minor reflection). For acoustic-gravity waves, the shoaling scenario is very different. In the case of a rigid bottom: (i) their group-velocity $c_{g,n}$ is real and decreases with the decrease of depth until it reaches zero at some finite depth h_{rn}, Eq. (29); (ii) their phase-velocity c_n is real and increases with the decrease of depth tending to infinity at the same depth h_{rn} (for depths smaller than h_{rn}: c_n and the wavenumber k_n are imaginary). In mathematical terms, the point x_{rn}, for which $h(x_{rn}) = h_{rn}$, is a *turning point*, which causes complete reflection, and requires special mathematical treatment; to be discussed in some detail in the Appendix. However, the physical picture for acoustic-gravity waves shoaling over a more realistic elastic ground is very different, and will be clarified in the sequel.

As previously stated, the energy flux is given by

$$F = c_g E, \tag{31}$$

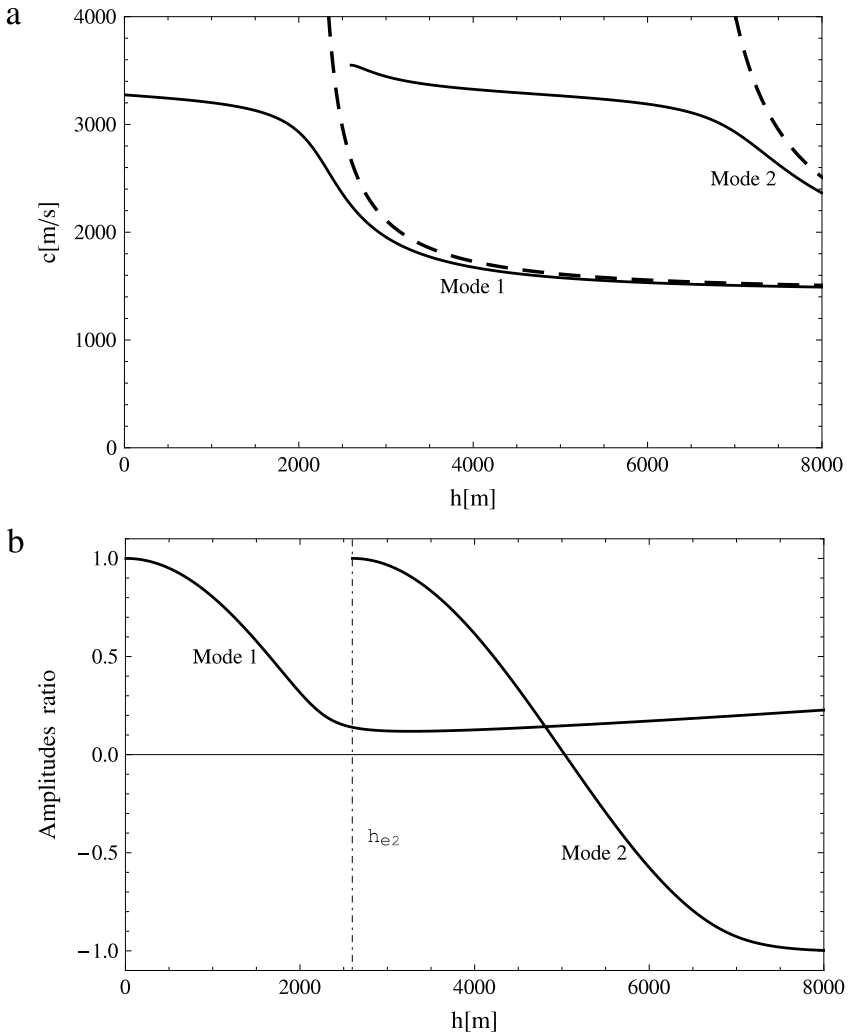

Fig. 3. Progressive acoustic-gravity modes with a frequency 0.167 Hz. (a) variation of phase-velocity with depth. (b) variation of the ratio of the ground-amplitude to the free-surface-amplitude as a function of the water depth. Dashed curves: rigid bottom; solid curves: elastic bottom.

where the group-velocity

$$c_g = \frac{\mathrm{d}\omega}{\mathrm{d}k}, \tag{32}$$

and the energy density

$$E = \frac{\rho_l}{L}\int_0^L \mathrm{d}x \int_{-h}^0 \mathrm{d}z(\dot{u}_l^2 + \dot{w}_l^2) + \frac{\rho_s}{L}\int_0^L \mathrm{d}x \int_{-\infty}^{-h} \mathrm{d}z(\dot{u}_s^2 + \dot{w}_s^2). \tag{33}$$

In (33) L is the wavelength, given by $L = 2\pi/k$; and the principle of equal-partition of kinetic and potential energies in conservative systems has been applied.

In Figs. 5(a) and 6(a) we present the variation of the group-velocities as function of water depth for $\omega = 1$ Hz and $\omega = 0.167$ Hz, respectively. Note that for the rigid bottom the group-velocities are zero for h_{rn}, $n = 1, 2, \ldots$, in contrast to the group-velocities for the elastic-bottom, which are non-zero and finite everywhere.

The variations of the energy density divided by A^2, (E/A^2), as function of depth is given in Figs. 5(b) and 6(b). From these figures one can see that E/A^2 for the rigid-bottom is finite for any depth, whereas for elastic-bottoms it tends to infinity at h_{en}, $n = 2, 3, \ldots$.

Assuming a constant energy flux, Eq. (31) enables to calculate the amplification factor A/A_0, where A_0 is the amplitude at the depths of 4000 m and 8000 m, for frequencies 1 Hz and 0.167 Hz, respectively. These calculations are presented in Figs. 7 and 8, which indicate the profound influence of the bottom structure. For a rigid bottom the shoaling waves attain infinitely large amplitudes at the turning points h_{rn}, $n = 1, 2, \ldots$. This physically unrealistic result is amendable by an appropriate local solution, see Appendix. In contrast, for the elastic bottom the comparable modes propagate into much shallower water, until they penetrate infinitely deep into the elastic media, and "disappear" with zero amplitude at h_{en}, $n = 2, 3, \ldots$. Most important is the Scholte wave which, as already mentioned, propagates all the way to the coast, and reaches its maximum amplification factor near h_{r1}. This amplification factor varies from 6 to 44, when the frequency is varied from 0.167 Hz to 1 Hz.

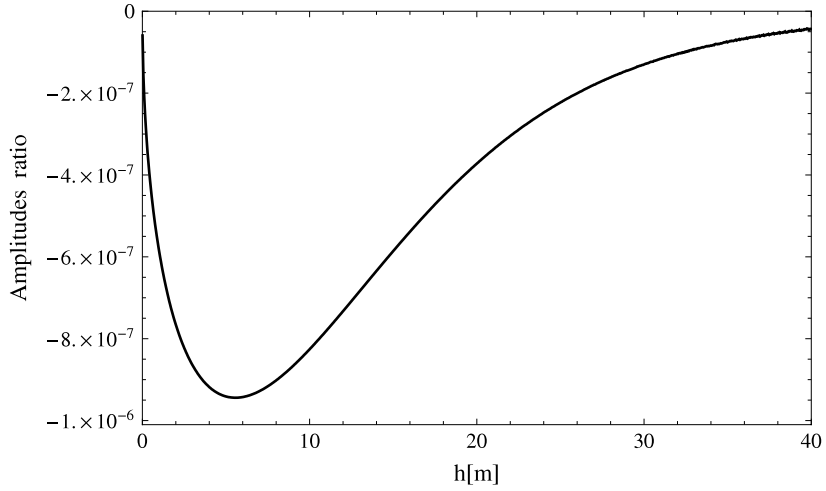

Fig. 4. The variation of the ratio of the ground-amplitude to the free-surface-amplitude for a gravity wave with frequency 0.167 Hz.

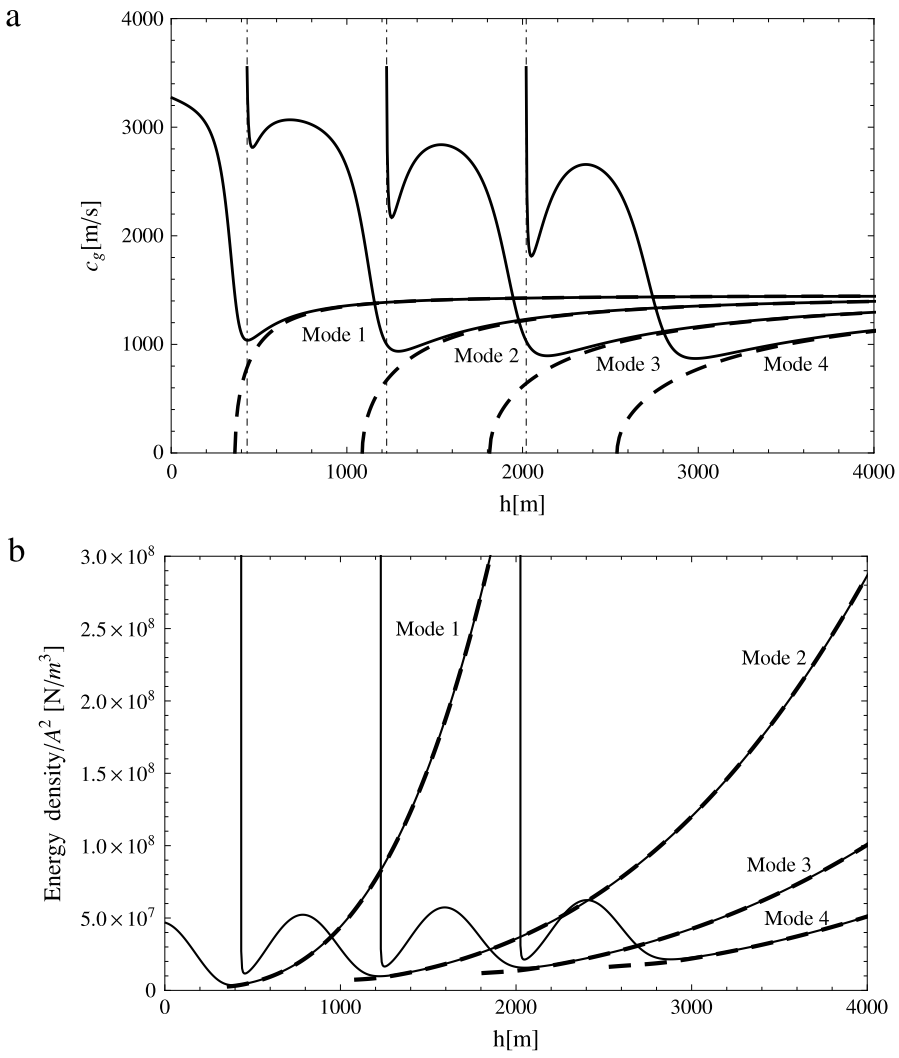

Fig. 5. Progressive acoustic-gravity modes with the frequency 1 Hz. Variation with depth of: (a) the group velocity; and (b) the ratio of the energy density to the square of the free-surface-amplitude. Dashed curves: rigid bottom; solid curves: elastic bottom.

6. Summary and conclusions

The main findings of this work are: (i) the dominance of the leading acoustic-gravity modes ($n = 1$) over the other modes ($n \geq 2$), and (ii) the ambiguous effect of the elasticity on this leading mode. The solution for the leading mode is only slightly

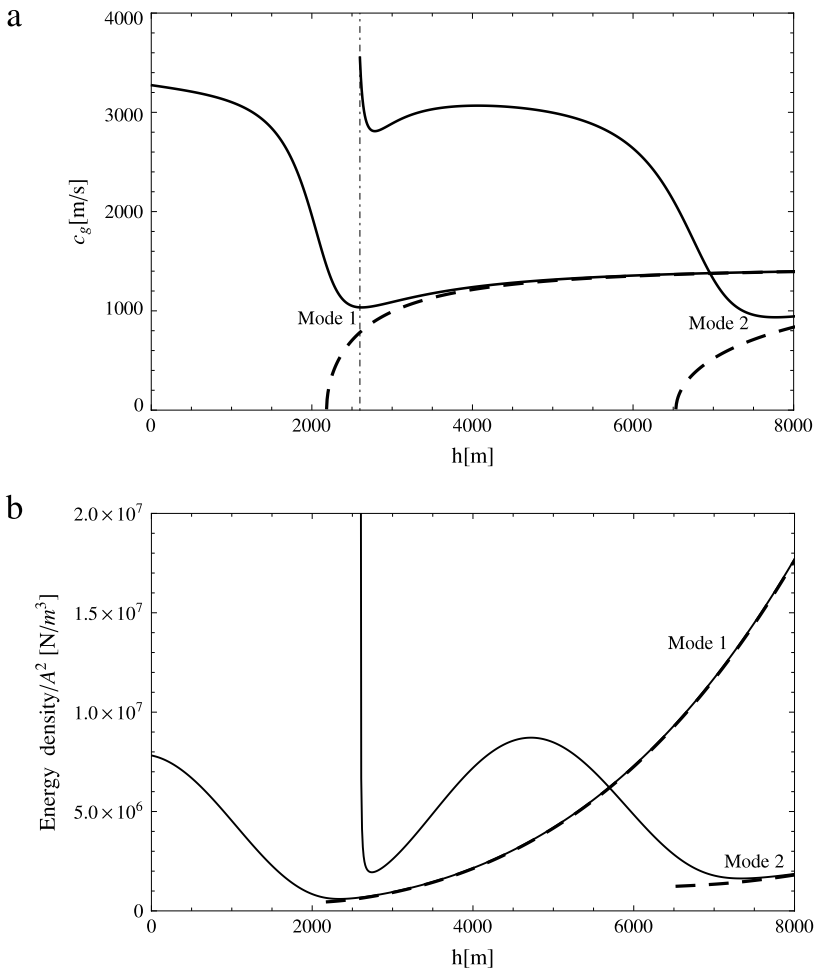

Fig. 6. Progressive acoustic-gravity modes with the frequency 0.167 Hz. Variation with depth of: (a) the group velocity; and (b) the ratio of the energy density to the square of the free-surface-amplitude. Dashed curves: rigid bottom; solid curves: elastic bottom.

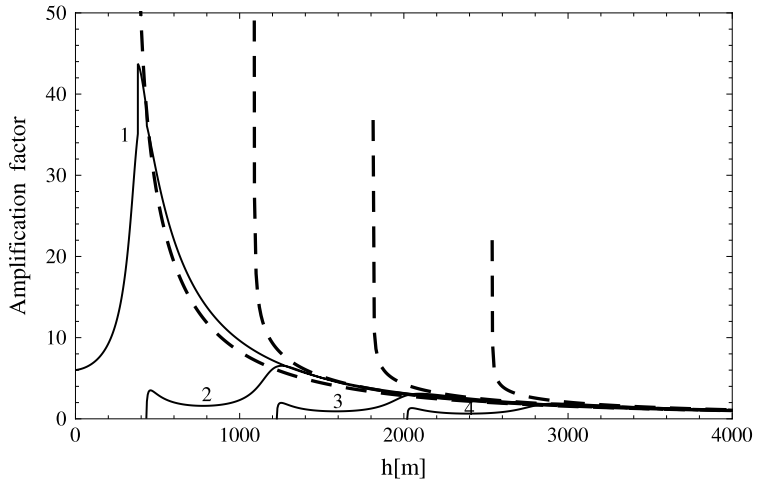

Fig. 7. Shoaling of acoustic-gravity mode with the frequency 1 Hz. Dashed curves: rigid bottom; solid curves: elastic bottom.

affected by the elasticity of the ground, as long as the water-depth is larger than h_{e2}. However, for water depths smaller than h_{r1} only the solution for an elastic ground, i.e. the so-called Scholte wave, outlasts. Another important finding is the fact that we can estimate the depth for which the acoustic-gravity wave attains its maximum intensity, as $h \in (h_{r1}, h_{e2})$. One may utilize this knowledge for defining the most suitable location of placing the measuring station for microseism study, as well as for the early detection of tsunamis. Note that for the acoustic-gravity waves on an elastic ground with $n \geq 2$ and $h < h_{en}$, a solution of the simple form (12a), (12b), (12c), which is based on separation of variables, does not exist; and that the study

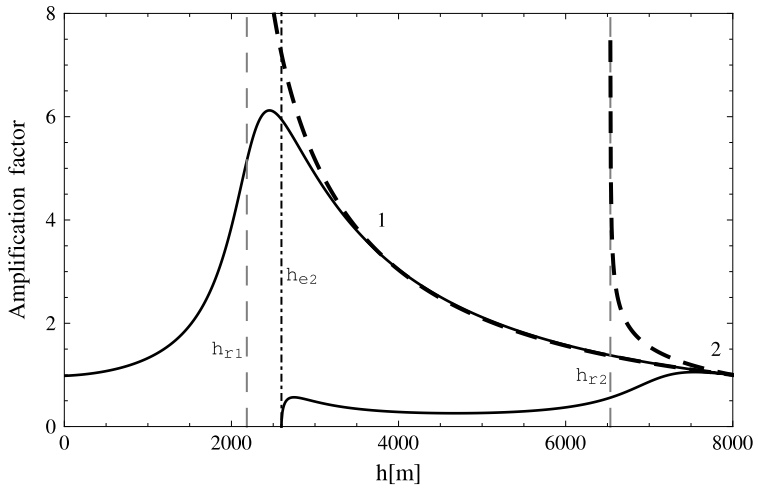

Fig. 8. Shoaling of acoustic-gravity mode with the frequency 0.167 Hz. Dashed curves: rigid bottom; solid curves: elastic bottom.

of the exact details by which the energy spreads within the liquid and elastic media, at $h < h_{en}$, $n \geq 2$, is beyond our current understanding.

Acknowledgments

This research was supported by the Israel Science Foundation (grant 63/09). The research is part of an M.Sc. thesis submitted by E. E. to Graduate School of the Technion—Israel Institute of Technology.

Appendix. Acoustic-gravity waves on a rigid bottom at the vicinity of h_{r1}

For a rigid bottom D_1 and D_2 of Eqs. (12a) and (12b) are zero, and Eq. (12c) for the liquid potential is replaced by

$$\phi_l = f(x)\frac{\cos[ir(h+z)]}{\cos(irh)}e^{-i\omega t}, \tag{A.1}$$

where $f(x)$ satisfies

$$\frac{\mathrm{d}^2 f(x)}{\mathrm{d}x^2} + k^2 f(x) = 0. \tag{A.2}$$

Note that far from the turning point the wavenumber k is regarded as a constant and $f(x) = \exp(ikx)$, whereas a Taylor expansion of k^2 is used at the vicinity of the turning point:

$$k^2 = k^2|_{h_0} + \left.\frac{\mathrm{d}(k^2)}{\mathrm{d}h}\right|_{h_0}(h-h_0) + \cdots \simeq -b_0 s_0 x, \tag{A.3}$$

where $h_0 \equiv h_{r1}$ is the water depth, and s_0 is the bottom slope at the turning point, and

$$b_0 = \frac{\pi^2}{2h_0^3}. \tag{A.4}$$

Substituting Eq. (A.3) into Eq. (A.2) leads to the Airy equation (Ai is the Airy function), and the final solution for the potential at the vicinity of h_{r1} is

$$\phi(x,z,t) = -\frac{2gA_0}{\omega}\frac{\beta_0\pi^{1/2}}{(b_0s_0)^{1/6}}\frac{\cos[ir(z+h)]}{\cos(irh)}\mathrm{Ai}\left((b_0s_0)^{1/3}x\right)\cos\left(\omega t+\frac{\pi}{4}\right). \tag{A.5}$$

The surface elevation is given by (11) as

$$\eta(x,t) = 2A_0\frac{\beta_0\pi^{1/2}}{(b_0s_0)^{1/6}}\mathrm{Ai}\left((b_0s_0)^{1/3}x\right)\sin\left(\omega t+\frac{\pi}{4}\right). \tag{A.6}$$

In (A.5) and (A.6) A_0 is the amplitude at the reference depth of 4000 m or 8000 m, for frequencies 1 Hz and 0.167 Hz, as before; and

$$\beta_0 = \frac{r_0}{r_R}\left(k_R\frac{\sin(2ir_0h_0)}{\sin(2ir_Rh_R)}\frac{\sin(2ir_Rh_R)+2ir_Rh_R}{\sin(2ir_0h_0)+2ir_0h_0}\right)^{1/2}. \tag{A.7}$$

The subscript 0 denotes values at the turning point, whereas the subscript R denotes values at the reference depth. Note that, the turning point causes complete wave reflection. The amplification factor at the turning point is given in Fig. A.9.

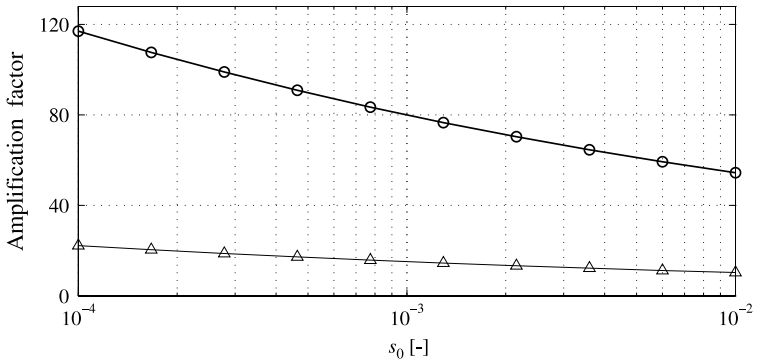

Fig. A.9. Effect of the seabed slope s_0 on the amplification factor at the turning point h_{r1}. The curves with circles and triangles denote a frequency of $f = 1.0$ and 0.167, respectively.

References

[1] F. Ardhuin, A. Balanche, E. Stutzmann, M. Obrebski, From seismic noise to ocean wave parameters: general methods and validation, J. Geophys. Res. 117 (2012) C05002. http://dx.doi.org/10.1029/2011JC007449.
[2] F. Ardhuin, E. Stutzmann, M. Schimmel, A. Mangeney, Ocean wave sources of seismic noise, J. Geophys. Res. 116 (2011) C09004. http://dx.doi.org/10.1029/2011JC006952.
[3] F.K. Duennebier, R. Lukas, E.-M. Nosal, J. Aucan, R.A. Weller, Wind, waves, and acoustic background levels at station ALOHA, J. Geophys. Res. 117 (2012) C03017. http://dx.doi.org/10.1029/2011JC007267.
[4] B. Levin, M. Nosov, Physics of Tsunamis, Springer-Verlag, Heidelberg, 2009, p. 327.
[5] M.S. Longuet-Higgins, A theory of the origin of microseisms, Philos. Trans. R. Soc. Lond. Ser. A 243 (1950) 1–35. http://dx.doi.org/10.1098/rsta.1950.0012.
[6] A.M. Dziewonshi, D.L. Anderson, Preliminary reference earth model, Phys. Earth Planet. Inter. 25 (1981) 297–356.
[7] S.C. Webb, The earth's 'hum' is driven by ocean waves over the continental shelves, Nature 445 (2007). http://dx.doi.org/10.1038/nature05536.
[8] J.G. Scholte, On true and psuedo Rayleigh waves, Proc. K. Ned. Akad. Wet. A 52 (1949) 652–653.
[9] M. Stiassnie, Tsunamis and acoustic-gravity waves from underwater earthquakes, J. Eng. Math. 67 (2010) 23–32.
[10] C.C. Mei, M. Stiassnie, D.K.-P. Yue, Theory and Applications of Ocean Surface Waves. Part 1: Linear Aspects, World Scientific Publishing Co. Pte Ltd., 2005, p. 506.